



Get Clarity On Generics

Cost-Effective CT & MRI Contrast Agents

**FRESENIUS
KABI**

[WATCH VIDEO](#)

AJNR






This information is current as
of August 7, 2025.

Rabbit Elastase Aneurysm Model Mimics the Recurrence Rate of Human Intracranial Aneurysms following Platinum Coil Embolization

Y.-H. Ding, S. Ghazy, D. Dai, W. Brinjikji, D.F. Kallmes
and R. Kadirvel

AJNR Am J Neuroradiol published online 28 April 2022
<http://www.ajnr.org/content/early/2022/04/28/ajnr.A7497>

Rabbit Elastase Aneurysm Model Mimics the Recurrence Rate of Human Intracranial Aneurysms following Platinum Coil Embolization

 Y.-H. Ding,  S. Ghozy,  D. Dai,  W. Brinjikji,  D.F. Kallmes, and  R. Kadirvel



ABSTRACT

BACKGROUND AND PURPOSE: Intracranial aneurysms treated with coils have been associated with incomplete occlusion, particularly in large or wide-neck aneurysms. This study aimed to validate the accuracy of the rabbit elastase model in predicting aneurysm recurrence in humans treated with platinum coils.

MATERIALS AND METHODS: Elastase-induced saccular aneurysms were induced in rabbits and embolized with conventional platinum coils. The recurrence rates of aneurysms were retrospectively analyzed. Morphologic characteristics of aneurysms, angiographic outcomes, and histologic healing were evaluated.

RESULTS: A total of 28 (15.3%) of 183 aneurysms recurred. The aneurysm recurrence rate observed in this study (15.3%) is similar to those reported in multiple analyses of aneurysm recurrence rates in humans (7%–27%). The rate of recurrence was higher in aneurysms treated without balloon assistance (19/66, 28.8%) compared with those treated with balloon assistance (9/117, 7.7%). Aneurysms treated with balloon-assisted coiling had a lower recurrence rate (OR = 0.17; 95% CI, 0.05–0.47; $P = .001$) and higher occlusion rate (OR = 6.88; 95% CI, 2.58–20.37; $P < .001$) compared with those treated without balloon-assisted coiling. In this rabbit elastase-induced aneurysm model, packing density and aneurysm volume were weak predictors of aneurysm recurrence; however, the packing density was a good predictor of the occlusion rate (OR = 1.05; 95% CI, 1.02–1.10; $P = .008$).

CONCLUSIONS: The rabbit elastase aneurysm model may mimic aneurysm recurrence rates observed in humans after platinum coil embolization. Moreover, balloon assistance and high packing densities were significant predictors of aneurysm recurrence and occlusion.

ABBREVIATIONS: CCA = common carotid artery; RCCA = right CCA

The prevalence of intracranial aneurysms in healthy adults is estimated to be 3%–5%.^{1,2} Endovascular embolization with platinum coils is the preferred treatment for unruptured and ruptured intracranial aneurysms because it is associated with lower morbidity and mortality rates compared with surgical clipping.^{3,4} However, coils have been associated with incomplete occlusion, leading to compaction and aneurysm recanalization, particularly in large aneurysms (diameter of ≥ 10 mm) or those with a wide

neck (>4 mm). The recurrence rate increases from 5% for aneurysms with a neck size between 4 and 10 mm to 20% for those with wider necks (>10 mm). Similarly, the recurrence rate of large aneurysms is 35%–50% compared with an overall recurrence rate of 20% in a heterogeneous population.^{5,6} To lower the recurrence rate of large and wide-neck aneurysms, a plethora of endovascular devices have been developed and tested in preclinical animal models.⁷


Preclinical trials of endovascular devices are necessary to evaluate their safety and efficiency. An ideal model requires aneurysm hemodynamic and histologic healing characteristics similar to those seen in humans. In models with surgical creation of aneurysms such as in both canine and rabbit venous pouch models, the presence of sutures at the aneurysm neck causes healing and fibrotic response, making it difficult to analyze healing after coil embolization. The canine venous pouch model, though widely used, cannot simulate the histologic and hemodynamic characteristics of humans.⁷ The swine model of intracranial aneurysms shows progressive occlusion and complete healing of aneurysms.⁸


Received October 7, 2021; accepted after revision March 9, 2022.

From the Department of Radiology, Mayo Clinic, Rochester, Minnesota.

Research reported in this publication was supported, in part, by the National Institutes of Health under Award Nos. R01NS076491, R43NS095455, U01NS089692, R01NS042646, and R21 HL072247.

Please address correspondence to Sherief Ghozy, MD, Mayo Clinic, Alfred Building 9-446, 200 First St. SW, Rochester, MN, 55905; e-mail: ghozy.sherief@mayo.edu; @SheriefGhozy; @WBrinjikji

 Indicates open access to non-subscribers at www.ajnr.org

 Indicates article with online supplemental data.

<http://dx.doi.org/10.3174/ajnr.A7497>

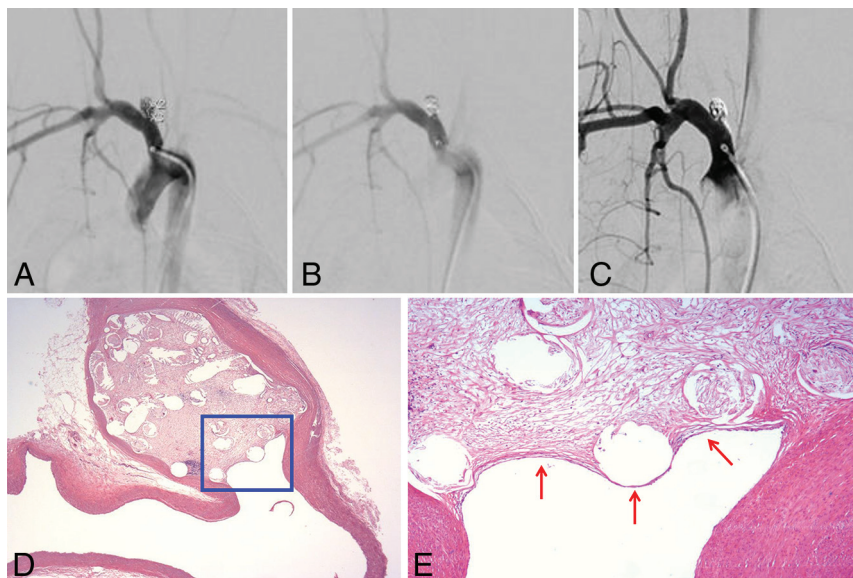


FIG 1. Angiographic and histopathologic evaluation of a completely occluded aneurysm on day 180. DSA images of the aneurysm before treatment (A), immediately after treatment showing complete occlusion (B), and before sacrifice demonstrating stable occlusion (C). Photomicrograph of an aneurysm section shows the aneurysm dome filled with organized connective tissue (D, H&E staining, original magnification $\times 12.5$) and the neck interface lined with a single layer of endothelium (arrows) (E, enlarged view of the box in D; H&E staining, original magnification $\times 40$).

This outcome makes the model irrelevant for testing aneurysm recurrence rates and the long-term efficiency of devices. In contrast, the rabbit aneurysm model has some advantages compared with clinical tissue. For instance, excising the aneurysm sac during the operation results in small segments of the aneurysm dome, while the rabbit model provides the opportunity to study the entire sac.⁹ Moreover, the rabbit model can be used to investigate the progressive wall degeneration of the aneurysm at multiple time points.⁹ Furthermore, the elastase-induced model has shown a similarity to the human intracranial aneurysm regarding geometric and hemodynamic aspects, including anatomy, size, long-term patency, and molecular characteristics.⁷ Nevertheless, as for all animal models, this model cannot account for the complex pathophysiology of human aneurysms, such as genetic predisposition, previous aneurysm history, comorbidities, wall inflammation, and individual life-style differences.

Typically, the elastase-induced aneurysm is created at the origin of right common carotid artery (RCCA) using a combination of open and endovascular techniques.¹⁰ Other modifications such as adjusting the position of the ligation, adjusting the position of the inflated balloon, injuring the aneurysm neck, and using the left common carotid artery (CCA) instead of the RCCA have been proposed as techniques to alter the volume, neck size, and configuration of the aneurysm, respectively.^{7,11–14} This model has been extensively used to study the healing response, occlusion rates, and recanalization rates after coil embolization. However, data are limited about the recurrence rate of aneurysms after platinum coil embolization in the rabbit elastase-induced aneurysm model. Therefore, the objective of this study was to evaluate the aneurysm recurrence rate in association with platinum coils in this aneurysm model.

MATERIALS AND METHODS

Rabbit Aneurysm Creation

Some of the rabbits used in this study were initially used as part of other investigations, in which we studied aneurysm healing mechanisms,¹⁵ developed a histologic healing scale,¹⁶ analyzed the relationship between aneurysm volume and healing,¹⁷ and compared the occlusion rates of platinum and modified coils.^{17,18} However, the original investigations were unrelated to this study. For this study, saccular aneurysms were created as described by Altes et al.¹⁰ By means of a sterile surgical technique, the RCCA was exposed to create a 1- to 2-mm beveled arteriotomy, and a 5F sheath was inserted retrograde in the midportion of the RCCA. Through this sheath, a 3F Fogarty balloon (Baxter Healthcare) was pushed to the origin of the RCCA and inflated to cause occlusion. Elastase (100 U/mL) mixed with equal amounts of iodinated contrast was intubated for 20 minutes, after which the balloon was deflated, the sheath was removed, and the RCCA was ligated. A 4-0 running

Vicryl suture (Ethicon) was used to close the skin before sending the rabbits to recovery.

Embolization Procedure

The embolization procedure was performed as described previously.¹⁸ Animals were anesthetized with the same procedure used during aneurysm creation. Under sterile conditions, the right common femoral artery was surgically exposed to place a 5F sheath and administer an injection of 500 U of heparin. Using the coaxial technique with continuous flushing with a heparin and normal saline solution, we advanced a 2 marker microcatheter into the aneurysm cavity. Radiopaque sizing devices were used to assess the size of the aneurysm during the 2D DSA. The aneurysm was embolized with ≥ 1 coil, depending on aneurysm diameter, and packing density was calculated as described in Herting et al.¹⁸ All the aneurysms were embolized as densely as possible using bare conventional platinum coils. A final control DSA was performed after coil placement and embolization, followed by removal of the catheters and sheath, ligation of femoral artery, and incision closure using a 4-0 Vicryl suture. Aneurysm occlusion was evaluated per the Raymond-Roy method: class 1, complete occlusion; class 2, near-complete occlusion; class 3, incomplete occlusion.¹⁹ We performed this evaluation on 2 occasions; postoperative and before sacrifice. We defined recanalization as any increased aneurysm filling in the follow-up angiography compared with the postoperative 2D DSA result. In contrast, recurrence was defined as a recurring or larger persistent filling defect on the follow-up angiography studies than the defect identified at the initial posttreatment and imaging (Figs 1 and 2).

Animal Sacrifice and Tissue Harvest

Angiographic follow-up was performed 15 days ($n = 23$), 1 month ($n = 100$), 1.5–2 months ($n = 9$), 3 months ($n = 8$), 4 months

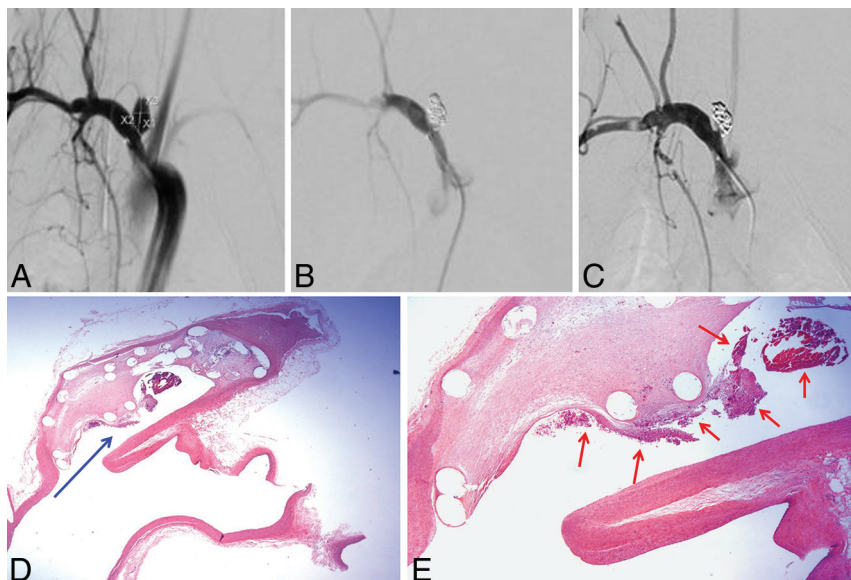


FIG 2. Angiographic and histopathologic evaluation of a recanalized aneurysm on day 180. DSA images of the aneurysm before treatment (A), immediately after treatment showing complete occlusion (B), and before sacrifice shows near-complete occlusion demonstrating recanalization (C). Photomicrograph of an aneurysm section shows a long, deep neck remnant that was wide open to parent artery connective tissue (D, H&E staining; original magnification $\times 12.5$). The tissue interface at the neck remnant appears to be macroconcave in relation to the tissues filled in the dome (D) and contains poorly organized thrombus (E, enlarged view of arrow in D; H&E staining, original magnification $\times 40$).

($n = 10$), and 6–12 months ($n = 33$) after embolization. DSA was performed after deeply anesthetizing the animals, and aneurysm occlusion was evaluated as described before: class 1, complete occlusion; class 2, near-complete occlusion; and class 3, incomplete occlusion.¹⁹ As described earlier, to determine the durability of the embolization posttreatment and follow-up, we categorized the angiograms into 3 categories: stable, recurrent, and progressive aneurysm.^{17,18} A lethal injection of pentobarbital was used to euthanize animals and harvest the aneurysms and parent arteries. The tissue samples were immediately fixed in 10% neutral buffered formalin.

Histologic Evaluation

Harvested tissue samples were processed as described by Dai et al.¹⁵ Samples were dehydrated in increasing concentrations of alcohol, followed by clearing with xylene. Specimens were embedded in paraffin blocks and sectioned in a coronal orientation at 1000- μm intervals using an IsoMet Low Speed saw (NCI MICRO).

Metallic coil fragments were removed under a dissecting microscope before re-embedding sections in paraffin blocks. These blocks were then sectioned at 4- μm intervals using a microtome with disposable blades. The sections were floated in a 42°C water bath, mounted on Superfrost Plus slides (Cardinal Health), and dried overnight in an oven at 37°C. Slides were deparaffinized and hydrated in water before staining with H&E. An ordinal grading system was used to evaluate histologic healing as described earlier.¹⁸ The total score was calculated by adding together the neck average, microcompaction score, and healing score.

Statistical Analysis

Categorical variables were presented as frequencies and percentages, with χ^2 tests (or the Fisher exact test) used for testing the difference. Continuous variables were expressed as means (SD), with testing differences evaluated using a t test or Mann-Whitney U test based on the data distribution (normally distributed or not). Logistic regression was used to identify any possible predictors of aneurysm recurrence and occlusion.

Regression results were expressed as ORs and 95% CIs. Receiver operating characteristic curves were also generated. The area under the curve was calculated; building the associated receiver operating characteristic curve to provide aggregate values of significant predictors correctly classified the occlusion status of each rabbit. All data were analyzed using R statistical and computing software (<http://www.r-project.org/software>), Version 4.1.1, using the “rcomdr” and “glm2” packages. $P < .05$ was considered significant for all statistical tests.

RESULTS

Aneurysm Characteristics

A total of 183 rabbits were included in this study (aneurysm characteristics are shown in Table 1), with a mean follow-up point of 2.3 (SD, 2.4) months, and balloon-assisted coiling was used in 63.9% (117/183) of aneurysms. Angiography before sacrifice showed complete occlusion in 79.8% of the subjects, while near-complete and incomplete occlusions were found in 11.5% and

Table 1: Characteristics of the included aneurysms

Variables	Balloon Used						P Value
	No		Yes		Total		
	Mean	SD	Mean	SD	Mean	SD	
Follow-up time point (mo)	3.1	2.2	1.8	2.4	2.3	2.4	<.001 ^a
Neck (mm)	3.8	5.0	2.8	1.2	3.2	3.1	.105
Width (mm)	3.7	1.0	3.6	1.0	3.6	1.0	.689
Height (mm)	8.2	2.2	7.9	2.4	8.0	2.3	.371
Volume (mm ³)	69.2	56.1	61.3	45.2	64.1	49.4	.676

Note:—SD, standard deviation.

^a Statistically significant.

Table 2: Summary of different outcomes following treatment

Variables	Balloon Used						P Value
	No		Yes		Total		
	Count	%	Count	%	Count	%	
Angio after treatment							
Complete	46	69.7	106	90.6	152	83.1	<.001 ^a
Incomplete	3	4.5	2	1.7	5	2.7	
Near-complete	17	25.8	9	7.7	26	14.2	
Angio before sacrifice							
Complete	41	62.1	105	89.7	146	79.8	<.001 ^a
Incomplete	13	19.7	3	2.6	16	8.7	
Near-complete	12	18.2	9	7.7	21	11.5	
Angio comparative score							
Progressive	3	4.5	6	5.1	9	4.9	<.001 ^a
Recurrence	19	28.8	9	7.7	28	15.3	
Stable	44	66.7	102	87.2	146	79.8	
Cross loop sign (coil bridging the neck)							
No	55	83.3	116	99.1	171	93.4	<.001 ^a
Yes	11	16.7	1	0.9	12	6.6	
Packing density (mean) (%)	24.8 (SD, 14.0)		30.5 (SD, 14.6)		28.5 (SD, 14.6)		.004 ^a
Total histologic healing score (mean)	5.6 (SD, 2.5)		5.4 (SD, 2.4)		5.5 (SD, 2.5)		.429

Note:—Angio indicates angiography; SD, standard deviation.

^a Statistically significant.

8.7% of the subjects, respectively. Comparing posttreatment angiographic occlusion with the presacrifice angiography showed a stable course in 79.8% of the subjects (146/183), recurrence in 15.3% (28/183), and a progressive course in 4.9%. The mean packing density was 28.5 (SD, 14.6), and the average histologic healing score was 5.5 (SD, 2.5). The recurrence rate was 7.7% (9/117) when a balloon was used compared with 28.8% (19/66) when a balloon was not used. The presence or absence of balloon-assisted coiling was a significant predictor of different outcomes (Table 2).

Predictors of Aneurysm Recurrence

Univariate and multivariate analyses of the potential predictors of the recurrence risk were performed. The predictors of recurrence risk identified by this method included follow-up time points, aneurysm characteristics (neck, width, height, volume), and balloon usage. The recurrence rate increased with lower packing density (OR = 0.95; 95% CI, 0.91–0.98; $P = .006$), wider neck diameters (OR = 1.75; 95% CI, 1.28–2.42; $P = .001$), higher aneurysm heights (OR = 1.36; 95% CI, 1.13–1.65; $P = .001$), larger aneurysm volumes (OR = 1.01; 95% CI, 1.00–1.02; $P = .010$), and the

absence of a balloon (OR = 0.21; 95% CI, 0.08–0.48; $P < .001$). In the multivariate model, only balloon usage (OR = 0.17; 95% CI, 0.05–0.47; $P = .001$) persisted as a significant predictor of recurrence (Table 3).

Predictors of Aneurysm Occlusion

Similarly, univariate and multivariate analyses of the potential predictors of the occlusion were performed. The occlusion rate was higher with narrower neck diameters (OR = 0.60; 95% CI, 0.44–0.80; $P = .001$), lower aneurysm heights (OR = 0.76; 95% CI, 0.64–0.90; $P = .002$), smaller aneurysm volumes (OR = 0.99; 95% CI, 0.99–1.00; $P = .039$), and the presence of a balloon (OR = 5.34; 95% CI, 2.50–11.95; $P < .001$). In the multivariate model, aneurysm width was significant (OR = 5.45; 95% CI, 1.54–19.76; $P = .008$), and only packing density (OR = 1.05; 95% CI, 1.02–1.10; $P = .008$) with balloon use (OR = 6.88; 95% CI, 2.58–20.37; $P < .001$) persisted as a significant predictor of recurrence (Table 4).

Packing Density Cutoff Values

Packing density cutoff values for predicting occlusion were obtained after analyzing the receiver operating characteristic

Table 3: Predictors of aneurysm recurrence^a

Predictors	Recurrence		OR (Univariable)	OR (Multivariable)
	No	Yes		
Packing density (mean) (%)	29.8 (14.6)	21.2 (12.2)	0.95 (0.91–0.98, P value = .006 ^b)	0.97 (0.93–1.01, P value = .129)
Follow-up time point (mean) (mo)	2.3 (2.5)	2.3 (2.0)	1.01 (0.84–1.18, P value = .887)	0.87 (0.67–1.11, P value = .297)
Neck (mean) (SD) (mm)	2.8 (1.2)	5.1 (7.4)	1.75 (1.28–2.42, P value = .001 ^b)	1.52 (0.99–2.37, P value = .054)
Width (mean) (SD) (mm)	3.6 (1.0)	3.8 (1.1)	1.30 (0.88–1.91, P value = .184)	0.27 (0.07–1.11, P value = .061)
Height (mean) (SD) (mm)	7.8 (2.2)	9.4 (2.6)	1.36 (1.13–1.65, P value = .001 ^b)	1.23 (0.91–1.71, P value = .191)
Volume (mean) (SD) (mm ³)	60.0 (44.1)	87.2 (68.8)	1.01 (1.00–1.02, P value = .010 ^b)	1.01 (0.98–1.05, P value = .354)
Balloon used (mean) (SD)				
No	47 (71.2)	19 (28.8)	Reference	
Yes	108 (92.3)	9 (7.7)	0.21 (0.08–0.48, P value <.001 ^b)	0.17 (0.05–0.47, P value = .001 ^b)

Note:—SD, standard deviation.

^a Model metrics: Akaike information criterion (AIC) = 135.5, C-statistic = 0.809, The Hosmer–Lemeshow test (H&L) = χ^2 (8) 4.62 ($P = .798$).

^b Statistically significant.

Table 4: Predictors of aneurysm occlusion^a

Predictors	Occlusion		OR (Univariable)	OR (Multivariable)
	No	Yes		
Packing density (mean) (SD) (%)	20.4 (11.9)	30.5 (14.5)	1.07 (1.03–1.11, <i>P</i> value < .001 ^b)	1.05 (1.02–1.10, <i>P</i> value = .008 ^b)
Follow-up time point (mean) (SD) (mo)	2.5 (2.1)	2.2 (2.5)	0.96 (0.84–1.12, <i>P</i> value = .576)	1.11 (0.89–1.42, <i>P</i> value = .398)
Neck (mean) (SD) (mm)	4.7 (6.5)	2.8 (1.1)	0.60 (0.44–0.80, <i>P</i> value = .001 ^b)	0.68 (0.45–1.02, <i>P</i> value = .065)
Width (mean) (SD) (mm)	3.7 (1.1)	3.6 (1.0)	0.89 (0.63–1.28, <i>P</i> value = .536)	5.45 (1.54–19.76, <i>P</i> value = .008 ^b)
Height (mean) (SD) (mm)	9.1 (2.5)	7.7 (2.2)	0.76 (0.64–0.90, <i>P</i> value = .002 ^b)	0.80 (0.60–1.05, <i>P</i> value = .123)
Volume (mean) (SD) (mm ³)	79.5 (65.1)	60.3 (44.1)	0.99 (0.99–1.00, <i>P</i> value = .039 ^b)	0.98 (0.96–1.01, <i>P</i> value = .229)
Balloon used (mean) (SD)				
No	25 (37.9)	41 (62.1)	Reference	
Yes	12 (10.3)	105 (89.7)	5.34 (2.50–11.95, <i>P</i> value < .001 ^b)	6.88 (2.58–20.37, <i>P</i> value < .001 ^b)

Note:—SD, standard deviation.

^a Model metrics: Akaike information criterion (AIC) = 146.3, C-statistic = 0.849, The Hosmer–Lemeshow test (H&L) = χ^2 (8) 11.22 (*P* = .190).

^b Statistically significant.

curve of all study subjects, which showed an overall good performance (area under the curve = 0.72). The values tested ranged from 6.00% to 93.94% (Online Supplemental Data). It appeared that values of $\geq 18\%$ had good sensitivity and specificity for predicting aneurysm occlusion; however, a packing density of 26.9% had the best balance of sensitivity, specificity, and positive and negative predictive values. On the basis of these findings, we reconducted the regression analyses categorizing packing density to $\geq 26.9\%$ and values to $< 26.9\%$. The univariable results showed no changes in the identified predictors from the previously built model, but it was not the case in the multivariate results, in which a packing density of $\geq 26.9\%$ and aneurysm width (millimeters) were significant predictors of higher occlusion rates (OR = 3.48; 95% CI, 1.31–10.15; *P* = .016; and OR = 4.96; 95% CI, 1.42–17.74; *P* = .012, respectively). On the other hand, larger aneurysm necks (millimeters) were associated with reduced occlusion rates (OR = 0.65; 95% CI, 0.43–0.97; *P* = .035) (Online Supplemental Data).

DISCUSSION

The aneurysm recurrence rate observed in this study (15.3%) is similar to those reported in multiple analyses of aneurysm recurrence rates in humans (7%–27%).^{20–26} We also observed that the rate of aneurysm recurrence was significantly reduced in procedures with balloon-assisted coiling and in aneurysms showing complete occlusion immediately after coil embolization. In this rabbit elastase-induced aneurysm model, packing density and aneurysm volume were weak predictors of aneurysm recurrence; however, the packing density was a good predictor of the occlusion rate. Previous effort had been made to compare the histologic changes in human cerebral aneurysms with the findings in animal models. A retrospective histopathologic evaluation of 27 elastase-induced aneurysms in rabbits was conducted,⁹ matching the findings to the 4-point scale described by Frösen et al.²⁷ The authors found similarities between the 2 models in terms of underlying aneurysm wall degeneration mechanisms such as lack of an intact elastic lamina, loss of the endothelium, and hypocellular aneurysm walls.⁹ In the elastase-induced model, the progression and distribution of the histologic subtypes of the aneurysm wall were similar to those previously described in the Frösen et al model.

Aneurysm recurrence is a significant limitation of endovascular coiling procedures, with recurrence rates reported as high as 50%.^{20–22,28–30} Additionally, large aneurysms and wide-neck aneurysms have been

identified as significant risk factors for early recurrence and are also vulnerable to early recurrence.³¹ In a single-center retrospective study, complete aneurysm occlusion was obtained in 31.7% of patients who underwent endovascular coiling procedures, and at ≤ 24 months, aneurysm recurrence occurred in 35.9% of this patient population.³² The study-level recurrence rate of the present study is comparable with that found in the human study, thus indicating the utility of the rabbit elastase model to mimic what is found in humans.

Aneurysm recurrence rates after coil embolization have been associated with different factors in humans. Aneurysms with a small neck have a lower recurrence rate compared with those with wider necks.²¹ Similarly, smaller aneurysms have a lower recurrence rate compared with large or giant aneurysms.^{21,22,33} Furthermore, the degree of aneurysm occlusion after treatment has also been related to recurrence. Aneurysms with initial complete occlusion were less likely to recur at follow-up.²² Our observation of a zero recurrence rate in aneurysms with complete occlusion is in line with this finding.

Aneurysm recurrence may occur through multiple mechanisms. Lower packing density or aneurysm growth may lead to coil compaction,³⁴ affecting histologic healing and subsequently causing aneurysm recanalization. In clinical settings, a large aneurysm volume is associated with low packing density and higher compaction rates. It is reported that a packing density of 24% is required to prevent compaction in aneurysms with a volume of < 600 mm.^{3,35} Our analysis showed that aneurysm volume and packing density were weak predictors of aneurysm recurrence. This result may be due to specific differences found in this model and to our embolization procedure. While it is known that the range in values of hemodynamic factors such as pressure, oscillatory shear index, and wall shear stress found in the rabbit elastase-induced aneurysm model is similar to that seen in humans,³⁶ the model is also known for its aneurysm patency. One report observed no changes in aneurysm geometry during 24 months.³⁷ The mean volume of aneurysms created in this study was less than that found in humans,³⁵ while the mean packing density was higher than 24%. A higher packing density has been associated with better histologic healing in the rabbit elastase aneurysm model.³⁸ This model also showed a mild biologic response, with studies reporting poor healing with the formation of loose connective tissue, the absence of contractile cells, and a lack of collagen deposition.^{15,39,40} In this rabbit elastase aneurysm model, the curvature of the parent vessel causes substantial inertia-driven flow, similar to that in humans, which may also contribute to aneurysm growth and recurrence.⁴¹

The development of more efficient endovascular devices for the treatment of intracranial aneurysms relies on preclinical testing in animal models. The rabbit aneurysm model has been considered a criterion standard for preclinical testing of various neurointerventional devices.^{17,42–45} Our results show that the aneurysm occlusion rates in rabbit aneurysms are comparable with those of human aneurysms following the use of endoluminal and intrasaccular flow-diverting devices,^{45,46} making this an ideal model for testing endovascular devices.

Limitations

Our study has limitations. The follow-up times in this study were limited to 1 year, which should be extended in future studies. Additionally, this is an extracranial aneurysm model with thick aneurysm walls, making it difficult to assess potential complications that may arise in treating human intracranial aneurysms.⁷ Moreover, our model has the inherent limitation of animal models, with their inability to account for all factors involved in the human complex pathophysiology, including various cellular phenotypes in the aneurysm wall. Although the coils were all of the same type, they were not the same brand and the operator was not the same in all cases, possibly introducing some bias. Finally, Raymond et al²² demonstrated that almost half of all recurrences were present by 6 months after coiling. Unfortunately, typical follow-up imaging of patients would be done at 3–6 months after coiling, but there is not much literature available to compare humans versus rabbits. We believe that evaluating the aneurysm occlusion stability and recurrence at early (<1 month), subchronic (1–3 months), and chronic (>3 months) stages would provide valuable insight into the timing of the recurrence.

CONCLUSIONS

The rabbit elastase aneurysm model may be a mosaic piece in the evaluation process of aneurysm treatments and may mimic aneurysm recurrence rates in humans. However, a comparative study against a human sample is necessary to confirm this finding.

ACKNOWLEDGMENTS

We would like to thank Duncan J. Maitland, PhD (Texas A&M University, College Station, Texas) for his effort to make this work possible.

Disclosure forms provided by the authors are available with the full text and PDF of this article at www.ajnr.org.

REFERENCES

1. Vlak MHM, Algra A, Brandenburg R, et al. **Prevalence of unruptured intracranial aneurysms, with emphasis on sex, age, comorbidity, country, and time period: a systematic review and meta-analysis.** *Lancet Neurol* 2011;10:626–36 [CrossRef Medline](#)
2. Imaizumi Y, Mizutani T, Shimizu K, et al. **Detection rates and sites of unruptured intracranial aneurysms according to sex and age: an analysis of MR angiography-based brain examinations of 4070 healthy Japanese adults.** *J Neurosurg* 2018;130:1–578 [CrossRef Medline](#)
3. Brinjikji W, Rabinstein AA, Nasr DM, et al. **Better outcomes with treatment by coiling relative to clipping of unruptured intracranial aneurysms in the United States, 2001–2008.** *AJNR Am J Neuroradiol* 2011;32:1071–75 [CrossRef Medline](#)
4. Qureshi AI, Vazquez G, Tariq N, et al. **Impact of International Subarachnoid Aneurysm Trial results on treatment of ruptured intracranial aneurysms in the United States: clinical article.** *J Neurosurg* 2011;114:834–41 [CrossRef Medline](#)
5. Spiessberger A, Vogt DR, Fandino J, et al. **Formation of intracranial de novo aneurysms and recurrence after neck clipping: a systematic review and meta-analysis.** *J Neurosurg* 2019;132:456–64 [CrossRef Medline](#)
6. Darflinger R, Thompson LA, Zhang Z, et al. **Recurrence, retreatment, and rebleed rates of coiled aneurysms with respect to the Raymond-Roy scale: a meta-analysis.** *J Neurointerv Surg* 2016;8:507–11 [CrossRef Medline](#)
7. Brinjikji W, Ding YH, Kallmes DF, et al. **From bench to bedside: utility of the rabbit elastase aneurysm model in preclinical studies of intracranial aneurysm treatment.** *J Neurointerv Surg* 2016;8:521–25 [CrossRef Medline](#)
8. Byrne JV, Hope JK, Hubbard N, et al. **The nature of thrombosis induced by platinum and tungsten coils in saccular aneurysms.** *AJNR Am J Neuroradiol* 1997;18:29–33 [Medline](#)
9. Wang S, Dai D, Kolumam Parameswaran P, et al. **Rabbit aneurysm models mimic histologic wall types identified in human intracranial aneurysms.** *J Neurointerv Surg* 2018;10:411–15 [CrossRef Medline](#)
10. Altes TA, Cloft HJ, Short JG, et al. **1999 ARRS Executive Council Award: creation of saccular aneurysms in the rabbit—a model suitable for testing endovascular devices.** *American Roentgen Ray Society. AJR Am J Roentgenol* 2000;174:349–54 [CrossRef Medline](#)
11. Ding YH, Dai D, Lewis DA, et al. **Can neck size in elastase-induced aneurysms be controlled? A prospective study.** *AJNR Am J Neuroradiol* 2005;26:2364–67 [Medline](#)
12. Ding YH, Dai D, Danielson MA, et al. **Control of aneurysm volume by adjusting the position of ligation during creation of elastase-induced aneurysms: a prospective study.** *AJNR Am J Neuroradiol* 2007;28:857–59 [Medline](#)
13. Wang K, Huang Q, Hong B, et al. **Neck injury is critical to elastase-induced aneurysm model.** *AJNR Am J Neuroradiol* 2009;30:1685–87 [CrossRef Medline](#)
14. Ding YH, Kadirvel R, Dai D, et al. **Creation of bifurcation-type elastase-induced aneurysms in rabbits.** *AJNR Am J Neuroradiol* 2013;34:E19–21 [CrossRef Medline](#)
15. Dai D, Ding YH, Danielson MA, et al. **Histopathologic and immunohistochemical comparison of human, rabbit, and swine aneurysms embolized with platinum coils.** *AJNR Am J Neuroradiol* 2005;26:2560–68 [Medline](#)
16. Dai D, Ding YH, Lewis DA, et al. **A proposed ordinal scale for grading histology in elastase-induced, saccular aneurysms.** *AJNR Am J Neuroradiol* 2006;27:132–38 [Medline](#)
17. Ding YH, Dai D, Lewis DA, et al. **Angiographic and histologic analysis of experimental aneurysms embolized with platinum coils, Matrix, and HydroCoil.** *AJNR Am J Neuroradiol* 2005;26:1757–63 [Medline](#)
18. Herting SM, Ding Y, Boyle AJ, et al. **In vivo comparison of shape memory polymer foam-coated and bare metal coils for aneurysm occlusion in the rabbit elastase model.** *J Biomed Mater Res B Appl Biomater* 2019;107:2466–75 [CrossRef Medline](#)
19. Roy D, Milot G, Raymond J. **Endovascular treatment of unruptured aneurysms.** *Stroke* 2001;32:1998–2004 [CrossRef Medline](#)
20. Ferns SP, Sprengers ME, van Rooij WJ, et al. **Coiling of intracranial aneurysms: a systematic review on initial occlusion and reopening and retreatment rates.** *Stroke* 2009;40:e523–29 [CrossRef Medline](#)
21. Murayama Y, Nien YL, Duckwiler G, et al. **Guglielmi Detachable Coil embolization of cerebral aneurysms: 11 years' experience.** *J Neurosurg* 2003;98:959–66 [CrossRef Medline](#)
22. Raymond J, Guilbert F, Weill A, et al. **Long-term angiographic recurrences after selective endovascular treatment of aneurysms with detachable coils.** *Stroke* 2003;34:1398–1403 [CrossRef Medline](#)

23. Cognard C, Weill A, Spelle L, et al. **Long-term angiographic follow-up of 169 intracranial berry aneurysms occluded with detachable coils.** *Radiology* 1999;212:348–56 [CrossRef Medline](#)
24. Tan IY, Agid RF, Willinsky RA. **Recanalization rates after endovascular coil embolization in a cohort of matched ruptured and unruptured cerebral aneurysms.** *Interv Neuroradiol* 2011;17:27–35 [CrossRef Medline](#)
25. Nguyen TN, Hoh BL, Amin-Hanjani S, et al. **Comparison of ruptured vs unruptured aneurysms in recanalization after coil embolization.** *Surg Neurol* 2007;68:19–23 [CrossRef Medline](#)
26. Marbacher S, Niemelä M, Hernesniemi J, et al. **Recurrence of endovascularly and microsurgically treated intracranial aneurysms—review of the putative role of aneurysm wall biology.** *Neurosurg Rev* 2019;42:49–58 [CrossRef Medline](#)
27. Frösien J, Piippo A, Paetau A, et al. **Remodeling of saccular cerebral artery aneurysm wall is associated with rupture: histological analysis of 24 unruptured and 42 ruptured cases.** *Stroke* 2004;35:2287–93 [CrossRef](#)
28. Consoli A, Vignoli C, Renieri L, et al. **Assisted coiling of saccular wide-necked unruptured intracranial aneurysms: stent versus balloon.** *J Neurointerv Surg* 2016;8:52–57 [CrossRef Medline](#)
29. Chung EJ, Shin YS, Lee CH, et al. **Comparison of clinical and radiologic outcomes among stent-assisted, double-catheter, and balloon-assisted coil embolization of wide neck aneurysms.** *Acta Neurochir (Wien)* 2014;156:1289–95 [CrossRef Medline](#)
30. Pötin M, Biondi A, Sourour N, et al. **The LUNA aneurysm embolization system for intracranial aneurysm treatment: short-term, mid-term and long-term clinical and angiographic results.** *J Neurointerv Surg* 2018;10:e34 [CrossRef Medline](#)
31. Mortimer AM, Marsh H, Klimczak K, et al. **Is long-term follow-up of adequately coil-occluded ruptured cerebral aneurysms always necessary? A single-center study of recurrences after endovascular treatment.** *J Neurointerv Surg* 2015;7:373–79 [CrossRef Medline](#)
32. Colby GP, Paul AR, Radvany MG, et al. **A single center comparison of coiling versus stent assisted coiling in 90 consecutive paraophthalmic region aneurysms.** *J Neurointerv Surg* 2012;4:116–20 [CrossRef Medline](#)
33. Gruber A, Killer M, Bavinszki G, et al. **Clinical and angiographic results of endosaccular coiling treatment of giant and very large intracranial aneurysms: a 7-year, single-center experience.** *Neurosurgery* 1999;45:793–804 [CrossRef Medline](#)
34. Hope JK, Byrne JV, Molyneux AJ. **Factors influencing successful angiographic occlusion of aneurysms treated by coil embolization.** *AJNR Am J Neuroradiol* 1999;20:391–99 [Medline](#)
35. Sluzewski M, van Rooij WJ, Slob MJ, et al. **Relation between aneurysm volume, packing, and compaction in 145 cerebral aneurysms treated with coils.** *Radiology* 2004;231:653–58 [CrossRef Medline](#)
36. Zeng Z, Kallmes DF, Durka MJ, et al. **Hemodynamics and anatomy of elastase-induced rabbit aneurysm models: similarity to human cerebral aneurysms?** *AJNR Am J Neuroradiol* 2011;32:595–601 [CrossRef Medline](#)
37. Ding YH, Dai D, Lewis DA, et al. **Long-term patency of elastase-induced aneurysm model in rabbits.** *AJNR Am J Neuroradiol* 2006;27:139–41 [Medline](#)
38. Ding YH, Dai D, Kadirvel R, et al. **Relationship between aneurysm volume and histologic healing after coil embolization in elastase-induced aneurysms: a retrospective study.** *AJNR Am J Neuroradiol* 2008;29:98–101 [CrossRef Medline](#)
39. Kallmes DF, Fujiwara NH, Yuen D, et al. **A collagen-based coil for embolization of saccular aneurysms in a New Zealand white rabbit model.** *AJNR Am J Neuroradiol* 2003;24:591–96 [Medline](#)
40. Dai D, Ding YH, Kadirvel R, et al. **A longitudinal immunohistochemical study of the healing of experimental aneurysms after embolization with platinum coils.** *AJNR Am J Neuroradiol* 2006;27:736–41 [Medline](#)
41. Meng H, Wang Z, Kim M, et al. **Saccular aneurysms on straight and curved vessels are subject to different hemodynamics: implications of intravascular stenting.** *AJNR Am J Neuroradiol* 2006;27:1861–65 [Medline](#)
42. Ding YH, Lewis DA, Kadirvel R, et al. **The Woven EndoBridge: a new aneurysm occlusion device.** *AJNR Am J Neuroradiol* 2011;32:607–11 [CrossRef Medline](#)
43. Kwon SC, Ding YH, Dai D, et al. **Preliminary results of the LUNA aneurysm embolization system in a rabbit model: a new intrasaccular aneurysm occlusion device.** *AJNR Am J Neuroradiol* 2011;32:602–06 [CrossRef Medline](#)
44. Kallmes DF, Ding YH, Dai D, et al. **A second-generation, endoluminal, flow-disrupting device for treatment of saccular aneurysms.** *AJNR Am J Neuroradiol* 2009;30:1153–58 [CrossRef Medline](#)
45. Kallmes DF, Ding YH, Dai D, et al. **A new endoluminal, flow-disrupting device for treatment of saccular aneurysms.** *Stroke* 2007;38:2346–52 [CrossRef Medline](#)
46. Rouchaud A, Brinjikji W, Ding YH, et al. **Evaluation of the angiographic grading scale in aneurysms treated with the WEB device in 80 rabbits: correlation with histologic evaluation.** *AJNR Am J Neuroradiol* 2016;37:324–29 [CrossRef Medline](#)